Synthesis of superhard materials

by Vladimir L. Solozhenko[†] and Eugene Gregoryanz[‡]

The study of solids at high pressures and temperatures is an important area of modern condensed matter physics, chemistry, and materials science. The last decade has seen revolutionary developments in the field of high-pressure experimentation: new types of cells allow a wider range of experiments at higher pressures, and third-generation synchrotrons have brought the possibility of conducting X-ray diffraction experiments that were unthinkable only 10 years ago. In this review, we give some recent examples to illustrate how modern high-pressure tools, such as the diamond anvil cell (DAC), multianvil press, and shock compression, can be used to answer questions relevant to the synthesis of new advanced materials. Our examples will be related mostly to superhard materials.

[†]LPMTM-CNRS, Institut Galilée,
Université Paris Nord,
93430 Villetaneuse, France
E-mail: vls@lpmtm.univ-paris13.fr

[‡]LMCP, IPGP, Université Paris 7,
75015 Paris, France,
and School of Physics and Center for Science
at Extreme Conditions,
University of Edinburgh,
Edinburgh, EH9 3JZ, UK
E-mail: e.gregoryanz@ed.ac.uk

With recent advances in high-pressure techniques, it has become possible to achieve significant compression of densities. Such changes of density will undoubtedly lead to new and unexpected effects. Highly compressed solids reveal a broad variety of unusual phenomena, such as the metal-insulator transition[1-4], electronic isostructural transitions[5], unexpected behavior in melting curves[6,7], pressure-induced amorphization[8-10], as well as incommensurate and 'host-guest' structures[11,12].

The focus on extreme conditions is also fueled by industrial interest in the synthesis of new materials with potentially useful properties such as superhardness or superconductivity. Superhard materials can be defined as having a Vickers hardness H_V > 40 GPa. In addition to high hardness – the capability of a material to withstand imprinting or scratching with another material – superhard materials usually possess other unique properties, such as compressional strength, shear resistance, large bulk moduli, high melting temperature, chemical inertness, and high thermal conductivity. This combination of properties makes the materials highly desirable for a number of applications[13].

The design of novel materials with a hardness comparable to that of diamond (H_V = 115 GPa[14]) poses a considerable experimental challenge[15]. Recent experimental efforts to synthesize new superhard phases have been based on the assumption that hardness is determined primarily by elastic moduli: bulk modulus[16] (a measure of resistance to volume change created by applied pressure) and shear modulus[17] (a measure of resistance to reversible deformation upon

ISSN:1369 7021

shear). However, the latter is much more difficult to measure experimentally for many samples, especially those synthesized and studied at high pressures.

Superhard phases are traditionally expected to be compounds with short bond lengths, i.e. those made up of the light elements B, C, O, and N, and having high cohesive energies[18]. For example, cubic C_3N_4 was predicted[19] to have a bulk modulus of K_0 = 496 GPa, which is larger than that of diamond (K_0 = 446 GPa[20]), because of the short length and high covalency of the C–N bond. However, years of research have failed to synthesize the desired phase[21-23], and cubic boron nitride (cBN) remains the hardest light nitride (H_V = 62 GPa[24]) with a bulk modulus of K_0 = 377 GPa[25].

An alternative approach is to search for compounds that include heavier elements but have a high coordination number. Transition metal nitrides are predicted to have larger bulk moduli than their parent metals because of directional bonding introduced by N atoms in the lattice, except when such directional bonding is already present in the parent metal, e.g. W or Os[26]. This search has recently encountered some success, with the synthesis of two low-compressibility transition metal nitrides, δ-MoN (K_0 = 345 GPa)[27] and PtN (K_0 = 372 GPa)[28]. The bulk moduli of the parent metals are 267 GPa[29] for Mo and 274 GPa[30] for Pt.

Synthesis of new superhard phases in the B–C–N system

Recent results in the search for new superhard materials indicate that the synthesis of phases with a hardness exceeding that of diamond is very unlikely. It seems worthwhile, therefore, to refocus the search for new superhard phases on the synthesis of materials more useful than, rather than harder than, diamond. This could include phases that are expected to be thermally and chemically more stable than diamond, and harder than cBN.

The similar atomic sizes of B, C, and N, as well as the similar structures of carbon and boron nitride polymorphs (i.e. diamond and cBN), suggest that it might be possible to synthesize diamond-like phase(s) containing all three elements. However, data on the attempted synthesis of B–C–N dense phases reported by different authors[31-37] are contradictory. It is unclear whether the synthesis products are diamond-like solid solutions between carbon and boron nitride or just mechanical mixtures of highly dispersed diamond and cBN.

Here, we briefly review our recent results on high-pressure and high-temperature synthesis of new diamond-like B–C–N ternary phases by direct solid-state conversion of turbostratic (i.e. completely one-dimensionally disordered) graphite-like $(BN)_xC_{1-x}$ ($0.33 \leq x \leq 0.61$) solid solutions[38] using the laser-heated DAC, multianvil press, and shock compression.

Synthesis at static pressures

Phase transitions of graphite-like BN–C solid solutions at pressures up to 30 GPa and temperatures up to 3000 K have been studied using a laser-heated DAC and angle-dispersive X-ray diffraction with synchrotron radiation[39] (Fig. 1). A novel superhard phase *c*-BC_2N was synthesized at pressures >18 GPa and temperatures >2200 K by a direct solid-state

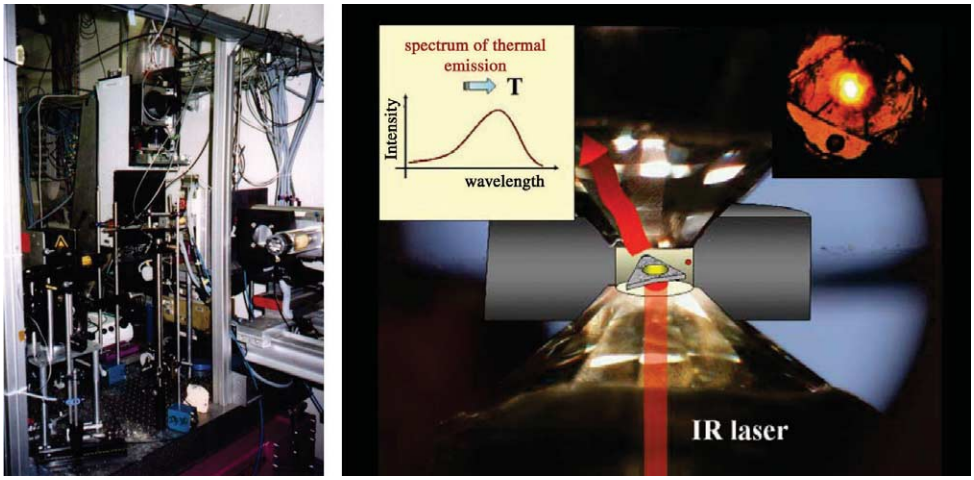

Fig. 1 (Left) The laser-heating system for monochromatic X-ray diffraction experiments at high pressures and temperatures at beamline ID30 of the European Synchrotron Radiation Facility. The main components of the system are a multimode yttrium-aluminum-garnet laser (λ = 1.064 μm), focusing optics to produce a large and homogenous heated area, an optical system for on-line temperature measurement, and a state-of-the-art diffraction setup. (Right) Schematic of the laser-heating technique in a DAC. The sample is placed in a pressure-transmitting medium between two diamond anvils and heated by an infrared laser.

phase transition of graphite-like $(BN)_{0.48}C_{0.52}$ (Fig. 2). The diffraction patterns of *c*-BC_2N exhibit only the *111*, *220*, and *311* Bragg lines of a cubic lattice, which correspond to the *Fd-3m* space group. The absence of the *200* line indicates

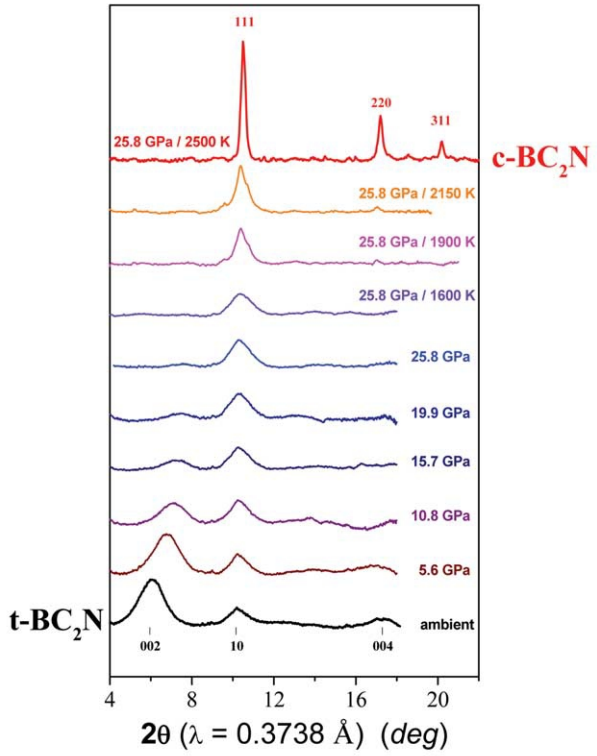

Fig. 2 Sequence of diffraction patterns taken at several pressures and temperatures during the synthesis of c-BC_2N[39]. Bottom and top patterns correspond to turbostratic BC_2N (t-BC_2N) and c-BC_2N, respectively. (Reprinted with permission from[39]. © 2001 American Institute of Physics.)

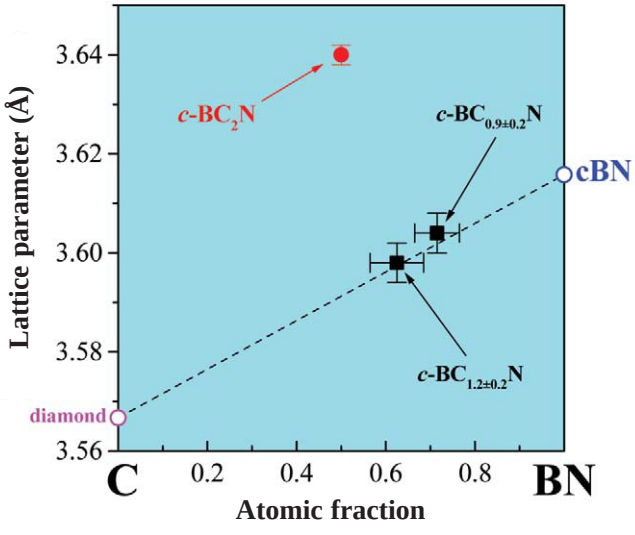

Fig. 3 Lattice parameters of c-BC_2N and diamond-like BN–C solid solutions. The dashed line represents ideal mixing between cBN and diamond. (Reprinted with permission from[54]. © Taylor & Francis.)

that the atomic scattering factors of two face-centered cubic (fcc) sublattices of the zincblende lattice are equal, which is possible only if B, C, and N atoms are uniformly distributed over both sublattices.

The lattice parameter of *c*-BC_2N at ambient conditions is a = 3.642 ± 0.002 Å, which is larger than those of both diamond (3.5667 Å) and cBN (3.6158 Å). The large deviation of the lattice parameter of *c*-BC_2N from the value expected from ideal mixing between diamond and cBN (Fig. 3) testifies that the synthesized phase is distinct from the so-called 'diamond/cBN alloys' reported earlier[31-37].

In order to measure the compressibility of *c*-BC_2N, a sample synthesized at 25.8 GPa and 3000 K was compressed up to 30 GPa at room temperature in the DAC[39]. The Birch equation of state was fitted to the data, giving values of K_0 = 282 ± 15 GPa and K_0' = 4.3 ± 1.1, with a zero-pressure cell volume of V_0 = 48.49 ± 0.08 $Å^3$. Therefore, the bulk modulus of *c*-BC_2N is smaller than the value of 420 GPa expected for ideal mixing between diamond and cBN.

Studies of the thermal stability of *c*-BC_2N in the 25-32 GPa pressure range using a laser-heated DAC at the ESRF, France show that the phase decomposes to form diamond and cBN at temperatures >2900 K[40].

We used a multianvil large-volume press to synthesize macroscopic (~2 mm^3) samples of *c*-BC_2N (Fig. 4)[41,42]. (The average size of samples synthesized in the DAC is 10^3 times smaller.) The sample was placed into a Pt capsule and subjected to experimental conditions of 25 GPa and 2200 K. Quenched samples were studied by X-ray diffraction using synchrotron radiation at HASYLAB-DESY, Germany. The diffraction patterns show the presence of a cubic phase with a lattice parameter of 3.640 ± 0.004 Å, which is very close to that of DAC-synthesized *c*-BC_2N. Electron microprobe analysis was carried out to examine the composition of the synthesized phase. From the full X-ray emission spectra of B, C, and N, the stoichiometry was determined to be BC_2N.

The granular structure of bulk *c*-BC_2N has been investigated by atomic force microscopy (AFM)[43]. The average size of grains observed in the AFM images is ~200 nm. The grains have a fine structure that can be attributed to small crystallites of 20-30 nm, which are combined into larger aggregates.

According to analytical transmission electron microscopy (ATEM)[44], the grain size of *c*-BC_2N ranges from 10 nm to 30 nm. The largest grains are of a regular cubic or tetrahedral

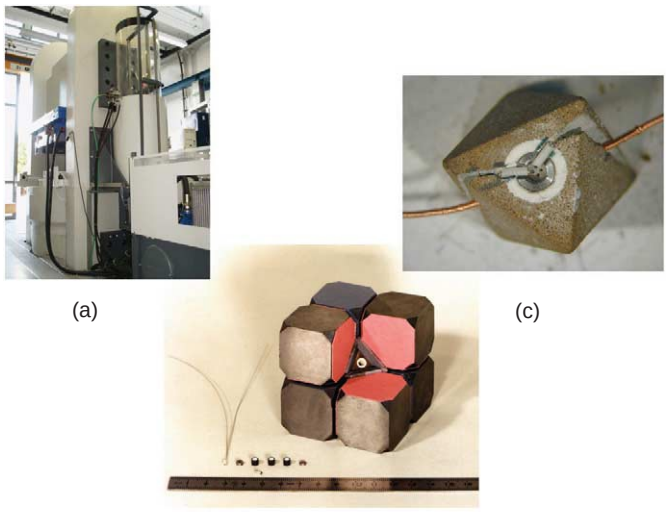

Fig. 4 Large-volume multianvil apparatus at the Bayerisches Geoinstitut[42]. This multianvil system is used with a hydraulic press (a) that can generate loads of up to 5000 tonnes. The six outer anvils define a cubic cavity of 100 mm edge length, in which eight second-stage 54 mm cubic inner anvils (b) are compressed. Experiments are performed using Cr_2O_3-doped MgO octahedral pressure cells (c) and pyrophyllite gaskets.

form, while fine grains are of a round form. Selected area electron diffraction (SAED) patterns exhibit rings corresponding to the *111*, *220*, and *311* reflections of the cubic phase. The absence of superstructure lines points to the statistically uniform distribution of B, C, and N atoms in the crystal lattice. Electron energy loss spectroscopy (EELS) of a *c*-BC_2N sample reveals characteristic peaks for sp^3-type atomic bonds, giving clear evidence for the formation of a diamond-like B–C–N ternary phase.

A broad Raman band corresponding to sp^3-coordinated atoms can be seen in spectra of *c*-BC_2N excited with ultraviolet (λ = 228.9 nm) and visible (λ = 488 nm) lasers[45]. The position of the Raman band was 1325.7 ± 1.6 cm^{-1} and can be attributed to a longitudinal optical (LO) mode of *c*-BC_2N. The large width of the observed Raman band (the full width at half maximum value is about 25 cm^{-1}) most likely reflects random substitution of C atoms in the diamond lattice by B and N.

The thermal stability of *c*-BC_2N in an Ar atmosphere at ambient pressure has been studied by X-ray diffraction with synchrotron radiation at LURE-DCI in France[46]. Our findings show that *c*-BC_2N remains stable up to 1800 K, and, hence, is characterized by a higher thermal stability than polycrystalline diamond with the same grain size.

The mechanical properties of *c*-BC_2N have been examined using micro- and nanoindentation[47]. The results are summarized in Table 1. The Vickers (H_V) and Knoop (H_K) hardnesses, as well as the nanohardness (H_N) of *c*-BC_2N, are intermediate between diamond and cBN, making the new phase the second hardest known material. The elastic recovery of *c*-BC_2N has been found to be 68%, which is higher than the corresponding value for cBN (60%) and approaches that of diamond. Based on nanohardness measurements, the value of the shear modulus for *c*-BC_2N is evaluated to be 447 ± 18 GPa, which is even higher than that of diamond. Brillouin scattering measurements[49] provide evidence that the nanocrystalline *c*-BC_2N is elastically isotropic. We were able to calculate the bulk and shear moduli as K_0 = 259 ± 22 GPa and G = 238 ± 8 GPa, respectively. The shear modulus value of G = 447 GPa evaluated from nanohardness measurements[47] is most likely an overestimate because of distinct deformation of the diamond indenter. At the same time, we find good agreement between the obtained bulk modulus and the corresponding value found in our compressibility measurements[39].

These results suggest that the new *c*-BC_2N phase has an unusual combination of mechanical properties. Its elastic moduli measured by Brillouin scattering and X-ray diffraction are lower than those of cBN, whereas its hardness measured independently by micro- and nanoindentation techniques is higher than that of single-crystal cBN and only slightly lower than that of diamond.

A laser-heated DAC enabled synthesis of the new superhard phase *c*-BC_2N, and use of the multianvil apparatus allowed us to synthesize macroscopic samples of polycrystalline *c*-BC_2N. Because of its extremely high

Table 1 *Hardness and elastic moduli of superhard diamond-like phases of the B–C–N system.*

	H_V (GPa)	H_K (GPa)	H_N (GPa)	K_0 (GPa)	G (GPa)
c-BC_2N	76[47]	55[47]	75[47]	282[39]	238[49]
c-BCN		52[55]		412[40]	
cBN	62[47]	44[47]	55[47]	377[25]	378[50]
Diamond	115[14]	63[48]		446[20]	538[51]

hardness and elastic recovery, as well as its high thermal stability, *c*-BC_2N holds promise as a potential superabrasive.

Shock-compression synthesis

The shock-compression synthesis of diamond-like B–C–N phases has been achieved by using cylindrical recovery containers with a ring gap that allow concentration of explosion energy in a given direction and multiple reflection of shock waves at the walls of the container[52]. The incident shock pressures on the samples are controlled through the choice of explosive. The use of a special additive to give a high shock temperature and a high compressibility allows sample heating up to 3500 K and abrupt cooling (10^8 K/s) on decompression.

Shock compression of graphite-like $(BN)_xC_{1-x}$ ($0.48 \le x \le 0.61$) solid solutions results in the formation of diamond-like phases. The proportion of these new phases in the recovered samples drastically increases with pressure and reaches 80 wt.% at 30 GPa. According to electron microprobe analysis, the stoichiometries of the diamond-like phases are $BC_{1.2\pm0.2}N$ and $BC_{0.9\pm0.2}N$ for the starting materials $(BN)_{0.48}C_{0.52}$ and $(BN)_{0.61}C_{0.39}$, respectively. Taking into account the considerable errors in determination of light elements, the stoichiometry of both diamond-like phases can be assumed to be BCN.

X-ray diffraction patterns of diamond-like BCN exhibit the *111*, *220*, and *311* lines of the cubic lattice, while the *200* line is missing. The latter indicates that B, C, and N atoms are statistically uniformly distributed over the crystal lattice as a result of the extremely high temperatures achieved in our experiments. From the profile analysis of the *220* and *311* lines of both *c*-BCN phases, it follows that the experimentally observed diffraction patterns are attributable to diamond-like BN–C uniform solid solutions, and not to a mechanical mixture of diamond and cBN.

Lattice parameters of *c*-$BC_{1.2\pm0.2}N$ and *c*-$BC_{0.9\pm0.2}N$ are 3.598 ± 0.004 Å and 3.604 ± 0.004 Å, respectively, and are in good agreement with values that would be expected from ideal mixing between diamond and cBN (Fig. 3). This clearly indicates that *c*-BCN phases synthesized in the present work have nothing to do with the cubic C–BN solid solutions reported earlier by Knittle *et al.*[34], which have lattice parameters that differ considerably.

According to ATEM studies[44], the mean grain size of both *c*-BCN phases is ~5 nm. The coarsest grains are of a tetrahedron habit, while fine grains are of a round shape. SAED patterns are fully consistent with diamond-like BN–C solid solutions. A superstructure was not observed, indicating that B, C, and N atoms are randomly distributed in the crystal lattice. The stoichiometry of the *c*-BCN phases estimated from EELS spectra was found to be BCN in both cases.

The shock-synthesized diamond-like BN–C solid solutions are heavily supersaturated as, under normal conditions, the solubility of C in cBN should not exceed several percent, according to theoretical analysis by Lambrecht and Segall[53].

The 300 K equation of state of *c*-$BC_{0.9\pm0.2}N$ was measured to 45 GPa using a DAC and energy-dispersive X-ray diffraction at HASYLAB-DESY[54]. The experimental pressure-volume data were fitted to the Birch-Murnaghan equation of state, giving K_0 = 412±9 GPa and K_0' = 4.3±1.1. The bulk modulus of *c*-BCN is higher, therefore, than that of cBN (K_0 = 377 GPa[25]) and the *c*-$C_{0.33}(BN)_{0.67}$ solid solution reported by Knittle *et al.*[34] (K_0 = 355 GPa), and is close to the 400 GPa value expected from ideal mixing between diamond and cBN. Thus, the diamond-like BN–C solid solution we synthesized has one of the largest bulk moduli known for any solid, being second only to that of diamond (K_0 = 446 GPa[20]).

A bulk *c*-BCN sample sintered at high pressures and temperatures from shock-synthesized *c*-$BC_{0.9\pm0.2}N$ powder has a Knoop hardness of 52 GPa[55], which is only slightly lower than that of *c*-BC_2N. In Fig. 5, we have plotted Knoop hardness against bulk modulus for the new diamond-like

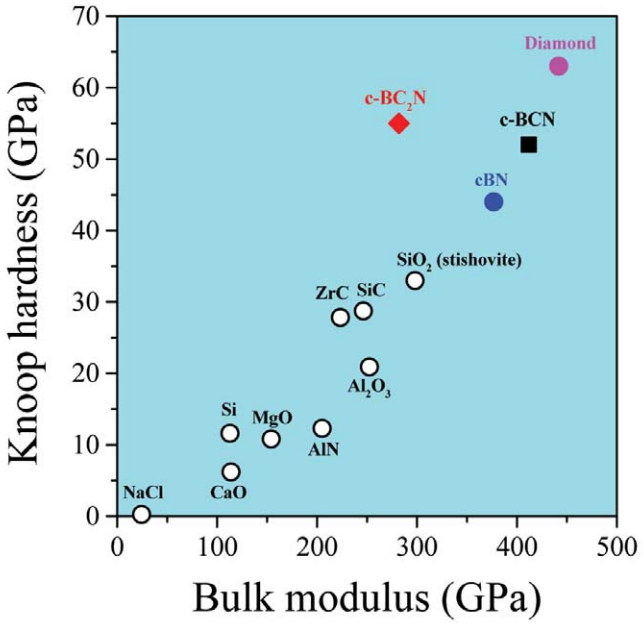

Fig. 5 Knoop hardness versus bulk modulus for the new diamond-like B–C–N phases and a common set of hard materials.

B–C–N phases[39,47,54,55], as well as a selection of other hard materials (H_K and K_0 values are taken from[17]).

Shock compression of nanopowders of graphite-like BN–C solid solutions has allowed the formation of an ideal cubic BN–C solid solution with a stoichiometry close to BCN and statistically uniform atomic distributions. This new *c*-BCN phase is characterized by very high bulk modulus and Knoop hardness values.

Low-compressibility metal nitrides

Molecular nitrogen has one of the strongest covalent bonds and, as a result, is very stable and inert under normal conditions. Yet nitrogen reacts with selected elements, forming compounds with a variety of properties[56,57]. Theoretical studies of nitrides are numerous, covering superconductivity[58], optoelectronic[59,60], and physical and structural properties[59,61,62]. One important group of these materials is the transition metal nitrides, which are mostly known for their superconducting properties[63-67].

Most transition metals form nitrides at high temperatures and at either ambient or high pressure (e.g. ZrN, VN, MoN). However, there are no known binary nitride compounds for the Sc, Mn, and Cu families of elements[68]. The Ni and Cu groups consist of metals with fcc structures that are stable over a wide pressure-temperature range[69]. Because of their structural simplicity and stability, most of the metals from these groups are used as pressure standards in DAC experiments, with Pt probably being the most often used (e.g.[70]). Pt forms simple binary compounds with halogens (e.g. PtF_4, PtI_2) and oxides and chalcogenides (e.g. PtO, PtS), but it is not known to form nitrides[68]. Among Ni, Pd, and Pt, only Ni has a nitride, Ni_3N[71].

There are number of ways to synthesize metal nitrides at ambient pressures. Synthesis can be achieved by chemical treatment at high temperature (>800 K), laser irradiation, or even mechanically, through plastic deformation of the surface[72]. Recently, a new nitride, platinum nitride, was synthesized at pressures up to 50 GPa using a laser-heated DAC technique[28]. This is one of the highest pressures at which synthesis has been carried out with complete recovery of the product at ambient conditions.

The reaction between Pt and N_2 was observed in Raman measurements following laser heating of samples to 2000 K at pressures >45 GPa (Fig. 6). At lower pressures, after numerous heatings, the transformation to the nitride phase was never observed. Above 45-50 GPa, the transition proceeds rapidly. The temperature of the transformation does not depend on pressure within the investigated pressure range (45-60 GPa). Previously, only reactions forming small molecules containing Pt and N in the gas phase have been reported (diatomic PtN by sputtering[73] and PtN, PtN_2, and $(PtN)_2$ by laser ablation[74]).

The Raman spectrum is striking, with strong LO and weaker transverse optical (TO) modes. Overall, it is similar to that of cubic GaN and InN, though the peaks are shifted in frequency as expected from mass effects[75,76]. On the other hand, the spectrum is much more intense, with both second- and third-order scattering also observed (Fig. 6).

After decompression, samples were recovered at ambient conditions and analyzed by an electron microprobe. Compositional profiles show that the Pt:N ratio is close to 1:1 but with some variations, i.e. PtN_{1-x} with $x < 0.05$. Pure Pt remains on the borders of the sample and also, to lesser degree, in the bulk. Micro-Raman spectra (measured using a laser spot size of ~5 μm) from all the sample grains studied are identical and consistent, with essentially no variation in stoichiometry. Moreover, the strength and width of the fundamental Raman bands are indicative of a highly crystalline and ordered structure.

The electron microprobe and Raman measurements mainly probe the surface of a sample (e.g. the electron microprobe

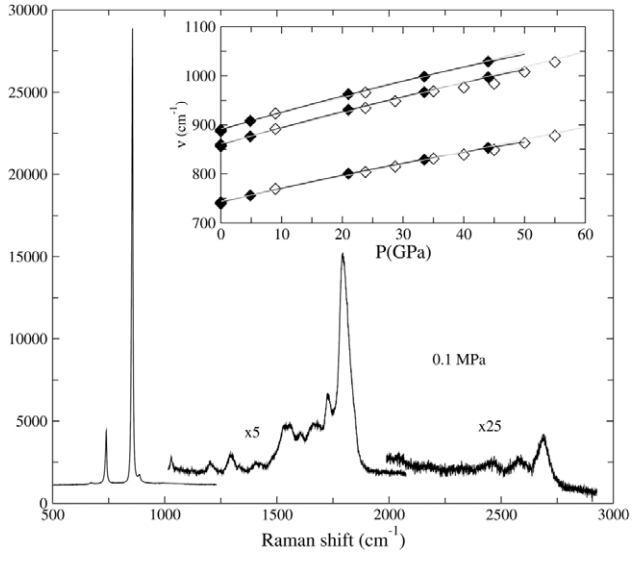

Fig. 6 Representative Raman spectra (with second- and third-order peaks) of platinum nitride measured at 0.1 MPa and 300 K after quenching from 55 GPa. Inset: the Raman shifts of platinum nitride as a function of pressure. Different symbols represent different experimental runs. Solid lines are guides for the eye only. (Reprinted with permission from[28]. © 2004 Nature Publishing Group.)

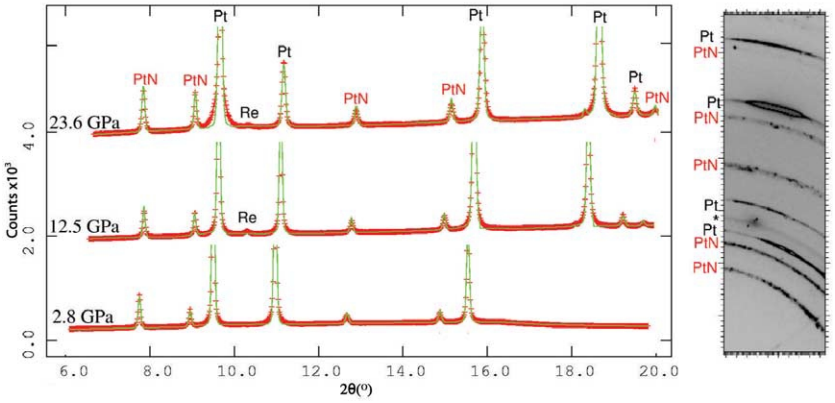

Fig. 7 In situ X-ray diffraction data. (Left) X-ray spectra of platinum nitride taken at different pressures. At ambient pressure, the spectrum was taken with λ = 0.3311 Å and others with λ = 0.3738 Å. Red crosses: data; green line: GSAS fit. (Right) Section of the CCD image at 28 GPa showing the powder-like texture; the asterisk indicates a Re diffraction ring. (Reprinted with permission from[28]. © 2004 Nature Publishing Group.)

samples a depth of ~1 μm at 5 kV). All microprobe measurements are indicative of either pure PtN or PtN with unreacted Pt, although it is possible that some nitrogen is dissolved in defects in unreacted zones. Recent theoretical studies[77,78] and our own *ab initio* simulations[79], together with X-ray photoelectron spectroscopy data[80], suggest that the stoichiometry of the platinum nitride is closer to 1:2 (Pt:N). This casts doubts on the reliability of microprobe measurements for the metal nitrides. It is likely that this error is a result of the penetration depth of the electron beam (1-2 μm) in microprobe measurements being much larger than the penetration depth of the nitride formation reaction (~100 nm). Microprobe measurements thus serve as a lower limit for nitrogen abundance in the newly formed compounds.

Synchrotron X-ray diffraction data were collected from two samples at pressures between ambient and 28 GPa (Fig. 7). Two-dimensional diffraction patterns were angularly integrated with the *Fit2D* program[81]. The lattice parameters of both Pt and platinum nitride phases were refined using the *GSAS* program package[82]. In the first loading, after formation of platinum nitride was confirmed by Raman scattering, X-ray data were collected at 28 GPa with the original N_2 as the pressure-transmitting medium. In the second run, the sample was recovered and reloaded with He as the pressure-transmitting medium. All the diffraction patterns at different pressures are consistent (Fig. 7), and platinum nitride can be indexed as a fcc structure at all pressures with a lattice parameter of a = 4.8041 ± 0.0002 Å at 0.1 MPa. The large mass difference between Pt and N does not allow the refinement of the N atom positions and the unambiguous determination of the space group. Further experiments where the N atom positions can be directly measured, e.g. neutron scattering, are required to answer these questions.

The evolution of platinum nitride volume with pressure was fitted to a Birch-Murnaghan equation of state. The resulting value for the bulk modulus of platinum nitride, K_0 = 372 ± 5 GPa, is about 100 GPa higher than pure Pt. The bulk modulus of PtN is comparable with that of cBN, K_0 = 377 GPa[25].

Theoretical calculations for transition metal nitrides[26] indicate that, in general, if the bulk modulus of the pure metal is large, it will be comparable for the corresponding nitride. The bulk modulus of platinum nitride is about 100 GPa higher than that of pure Pt. This enhancement probably arises from the strong directional Pt–N covalent bond with orbitals being close to half filled[26]. Formation of metal–nitrogen covalent bonds will ultimately result in the change of the electrical properties of Pt, making the new material semiconducting. All platinum nitride samples are lustrous and darker than pure Pt in reflected white light, and totally opaque in transmitted light. Using a magnetic-susceptibility technique[83], we looked for a superconducting transition at temperatures down to 2 K. The visual appearance and the absence of the superconducting signal suggest that platinum nitride is either a poor metal or a semiconductor with a small band gap. This is different from most of the other transition metal nitrides, which are known to be superconductors, e.g. VN and NbN.

Thus, using the DAC, we have synthesized and characterized a new nitride, PtN, which has a very high bulk modulus and a remarkable Raman scattering cross section.

Conclusions

These examples demonstrate the high-pressure synthesis of novel superhard phases using the modern high-pressure tools of DAC, multianvil press, and shock compression.

The complete recovery of synthesized products at ambient conditions holds promise for their eventual development as new technological materials. MT

REFERENCES

1. Reichlin, R., *et al., Phys. Rev. Lett.* (1986) **56** (26), 2858
2. Goettel, K. A., *et al., Phys. Rev. Lett.* (1989) **62** (6), 665
3. Eremets, M., *et al., Science* (1998) **281**, 1333
4. Eremets, M., *et al., Phys. Rev. Lett.* (2000) **85** (13), 2797
5. Badro, J., *et al., Phys. Rev. Lett.* (2002) **89**, 205504
6. Gregoryanz, E., *et al., Phys. Rev. Lett.* (2003) **90**, 175701
7. Gregoryanz, E., *et al., Phys. Rev. Lett.* (2005) **94**, 185502
8. Mishima, O., *et al., Nature* (1984) **310**, 393
9. Hemley R. J., *et al., Nature* (1989) **338**, 638
10. Gregoryanz, E., *et al., Phys. Rev. B* (2001) **64**, 052103
11. Nelmes, R. J., *et al., Phys. Rev. Lett.* (1999) **83** (20), 4081
12. McMahon, M., *et al., Phys. Rev. Lett.* (2000) **85** (23), 4896
13. Riedel, R., (ed.), *Handbook of Ceramic Hard Materials*, Wiley-VCH, Weinheim, (2000)
14. Novikov, N. V., and Dub, S. N., *J. Hard Mater.* (1991) **2**, 3
15. Haines, J., *et al., Annu. Rev. Mater. Res.* (2001) **31**, 1 (and references therein)
16. Legèr, J., and Haines, J., *Endeavor* (1997) **21**, 121
17. Teter, D. M., *MRS Bull.* (1998) **23** (1), 22
18. Brazhkin, V. V., *et al., Philos. Mag. A* (2002) **82** (2), 231
19. Teter, D. M., and Hemley, R. J., *Science* (1996) **271**, 53
20. Gillet, Ph., *et al., Phys. Rev. B* (1999) **60** (21), 14660
21. DeVries, R. C., *Mater. Res. Innovations* (1997) **1**, 161
22. Matsumoto, S., *et al., Diamond Relat. Mater.* (1999) **8** (7), 1175
23. Malkow, T., *Mater. Sci. Eng. A* (2001) **302** (2), 309
24. Novikov, N. V., *et al., Sov. J. Superhard Mater.* (1983) **5**, 16
25. Solozhenko, V. L., *et al., Appl. Phys. Lett.* (1998) **72** (14), 1691
26. Grossman, J., *et al., Phys. Rev. B* (1999) **60** (9), 6343
27. Soignard, E., *et al., Phys. Rev. B* (2003) **68**, 132101
28. Gregoryanz, E., *et al., Nat. Mater.* (2004) **3** (5), 294
29. Ming, L. C., and Manghani, M. H., *J. Appl. Phys.* (1978) **49** (1), 208
30. Dewaele, A., *et al., Phys. Rev. B* (2004) **70**, 094112
31. Badzian, A. R., *Mater. Res. Bull.* (1981) **16** (11), 1385
32. Nakano, S., *et al., Chem. Mater.* (1994) **6** (12), 2246
33. Kakudate, Y., *et al., Trans. Mater. Res. Soc. Jpn.* (1994) **14B**, 1447
34. Knittle, E., *et al., Phys. Rev. B* (1995) **51** (18), 12149
35. Nakano, S., In *Proceedings of the 3rd NIRIM International Symposium on Advanced Materials*, National Institute for Research in Inorganic Materials, Tsukuba, Japan (1996)
36. Kagi, H., *et al.*, In *Proceedings of the 15th International Association for the Advancement of High Pressure Science and Technology (AIRAPT) International Conference*, World Scientific, Singapore, (1996)
37. Komatsu, T., *et al., J. Mater. Chem.* (1996) **6**, 1799
38. Hubaček, M., and Sato, T., *J. Solid State Chem.* (1995) **114** (1), 258
39. Solozhenko, V. L., *et al., Appl. Phys. Lett.* (2001) **78** (10), 1385
40. Solozhenko, V. L., *High Pressure Res.* (2004) **24** (4), 499
41. Rubie, D. C., *Phase Transitions* (1999) **68**, 431
42. Frost, D. J., *et al., Phys. Earth Planet. Inter.* (2004) **143-144**, 507
43. Zinin, P. V., *et al., J. Mater. Sci.* (2005) **40** (11), 3009
44. Langenhorst, F., and Solozhenko, V. L., *Phys. Chem. Chem. Phys.* (2002) **4** (20), 5183
45. Hubble, H. W., *et al., J. Raman Spectrosc.* (2004) **35** (10), 822
46. Solozhenko, V. L., and Andrault, D., unpublished results
47. Solozhenko, V. L., *et al., Diamond Relat. Mater.* (2001) **10** (12), 2228
48. Brooks, C. A., In *Properties and Growth of Diamond*, INSPEC, London, (1994)
49. Tkachev, S. N., *et al., Phys. Rev. B* (2003) **68**, 052104
50. Manghnani, M. H., In Proceedings of the 5th NIRIM International Symposium on Advanced Materials, National Institute for Research in Inorganic Materials, Chichester, (1998)
51. McSkimin, H. J., *et al., J. Appl. Phys.* (1972) **43** (3), 985
52. Kurdyumov, A. V., *et al., Poroshk. Metall.* (1999) **11-12**, 88 (in Russian)
53. Lambrecht, W. R., and Segall, B., *Phys. Rev. B* (1993) **47** (15), 9289
54. Solozhenko, V. L., *High Pressure Res.* (2002) **22** (3-4), 519
55. Solozhenko, V. L., unpublished results
56. McMillan, P. F., *Nat. Mater.* (2002) **1** (1), 19
57. Zerr, A., *et al., Nature* (1999) **400**, 340
58. Papaconstantopoulos, D. A., *et al., Phys. Rev. B* (1985) **31** (2), 752
59. Ching, W., *et al., J. Am. Ceram. Soc.* (2002) **85** (1), 75
60. Dong, J., *et al., Phys. Rev. B* (2000) **61** (18), 11979
61. Kroll, P., *Phys. Rev. Lett.* (2003) **90**, 125501
62. Ching, W. Y., *et al., Phys. Rev. B* (2000) **61** (16), 10609
63. Pessal, N., *et al., J. Phys. Chem. Solids* (1968) **29**, 19
64. Pierson, H., In *Handbook of Refractory Carbides and Nitrides: Properties, Characteristics and Applications*, Noyes Publications, Westwood, (1996)
65. Luo, H. L., *et al., Phys. Rev. B* (1984) **29** (3), 1443
66. Zasadzinsky, J., *et al., Phys. Rev. B* (1985) **32** (5), 2929
67. Takamori, T., *et al., J. Appl. Phys.* (1990) **68** (5), 2192
68. Greenwood, N., and Earnshaw, A., In *Chemistry of the Elements*, Butterworth-Heinemann, UK, (1997)
69. Young, D., In *Phase Diagrams of Elements*, University of California Press, Berkeley, (1991)
70. Holmes, N. C., *et al., J. Appl. Phys.* (1989) **66** (7), 2962
71. Leineweber, A., *et al., Inorg. Chem.* (2001) **40** (23), 5818
72. Tong, W. P., *et al., Science* (2003) **299**, 686
73. Friedman-Hill, E. J., and Field, R. W., *J. Chem. Phys.* (1994) **100** (9), 6141
74. Cintra, A., *et al., J. Phys. Chem. A* (2001) **105** (33), 7799
75. Goñi, A. R., *et al., Phys. Rev. B* (2001) **64** (3), 35205
76. Tabata, A., *et al., Appl. Phys. Lett.* (1999) **74** (3), 362
77. Yu, R. and Zhang, X. F., *Appl. Phys. Lett.* (2005) **86**, 121913
78. Yu, R., *et al., Phys. Rev. B* (2005) **72,** 054103
79. Young, A., *et al.*, to be published
80. Crowhurst, J. C., *et al.*, In *Proceedings of the Joint 20th AIRAPT-43rd EHPRG International Conference on High Pressure Science and Technology*, Karlsruhe, (2005)
81. Hammersley, A., *Fit2D*, European Synchrotron Radiation Facility publication ESRF98HA01T (1996)
82. Larson, A., and Von Dreele, R., *GSAS manual*, Report LAUR 86-748, Los Alamos
83. Timofeev, Y., *et al., Rev. Sci. Instrum.* (2002) **73** (2), 371